Supplementary information

for

Sustainable Mechanochemical Growth of Double-Network Hydrogels

Supported by Vascular-like Perfusion

Gumi Wei[1], Yumeko Kudo[1], Takahiro Matsuda[1], Zhi Jian Wang[2], Qi Feng Mu[1], Daniel R. King[3], Tasuku Nakajima[2,3,*], and Jian Ping Gong[2,3,*]

([1] Graduate School of Life Science, Hokkaido University, [2] Institute for Chemical Reaction Design and Discovery (WPI-ICReDD), Hokkaido University, Sapporo 001-0021, Japan, [3] Faculty of Advanced Life Science, Hokkaido University, Sapporo 001-0021, Japan)

[1]Tel: +81-011-706-9011, E-mail: tasuku@sci.hokudai.ac.jp; gong@sci.hokudai.ac.jp

Chemicals

2-Acrylamido-2-methylpropane sulfonic acid sodium salt (NaAMPS, 49.8 wt. % aqueous solution) was provided by Toagosei. Acrylamide (AAm) was purchased from Junsei Chemical. *N,N'*-Methylenebisacrylamide (MBAA), ultraviolet (UV) initiator a-ketoglutaric acid (a-keto), ammonium iron(II) sulfate ($(NH_4)_2Fe^{II}(SO_4)_2$) hexahydrate, sulfuric acid (H_2SO_4), *N*-isopropylacrylamide (NIPAAm), 2-oxoglutaric acid, xylenol orange (XO), neutral red, and brilliant green were purchased from Wako Pure Chemical Industries. 8-Anilino-1-naphthalenesulfonic acid (ANS) was purchased from Tokyo Chemical Industry. All the reagents were used as received.

Mechanoradical concentration of DN gels measured by Fenton color reaction

The mechanoradical concentration in c-DN gels was determined by a method reported in our previous work[1, 2]. c-DN hydrogels were immersed in an aqueous solution of 100 μM $(NH4)_2Fe^{II}(SO_4)_2$, 100 μM XO and 20 mM H_2SO_4 for 1 day. Then gels were stretched to the preset strain ($\varepsilon_{max} = 7$) at a velocity of 100 mm min^{-1} and then immediately recovered to the initial position. After 30 mins, when no further color change was observed, the gels were cut with scissors to obtain the gauge part, which was then placed in a quartz optical cell (45 mm × 10 mm × 10 mm) for UV-visible absorption spectroscopy (UV-1800, Shimadzu Co.) measurement. To quantify the Fe^{3+} concentration, the calibration of our former work was used as the constitution is the same. By comparing the normalized absorbance at 580 nm of DN gels after stretching with the calibration curve, we can evaluate the Fe^{3+} concentration, which is assumed to be equal to the mechanoradical concentration.
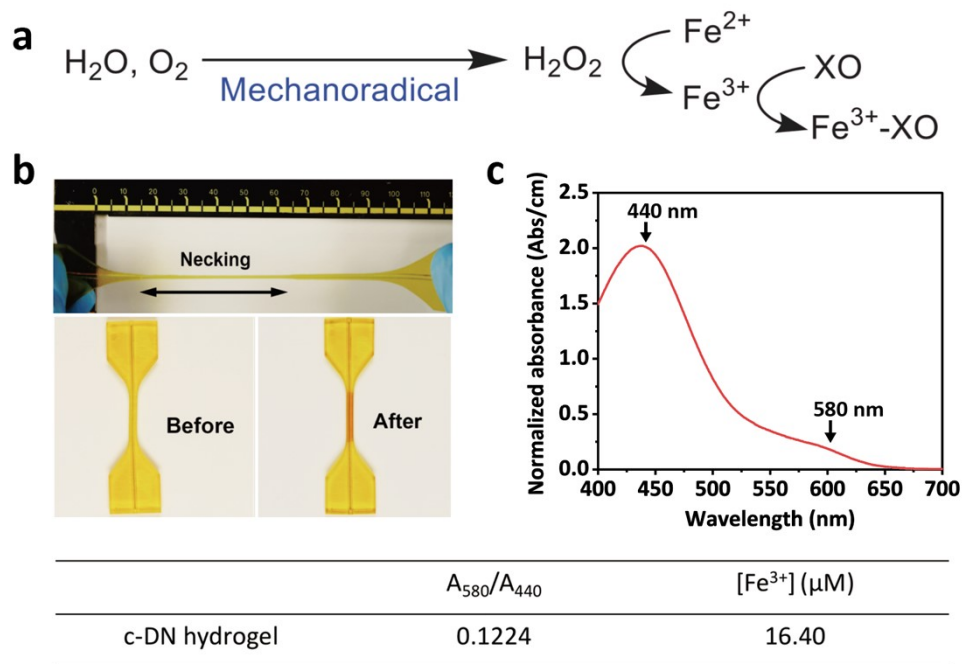
a Reaction scheme:

$$H_2O, O_2 \xrightarrow{\text{Mechanoradical}} H_2O_2 \xrightarrow{Fe^{2+}}{Fe^{3+}} \xrightarrow{XO} Fe^{3+}\text{-}XO$$

	A_{580}/A_{440}	$[Fe^{3+}]$ (µM)
c-DN hydrogel	0.1224	16.40

Figure S1. Quantification of Fe^{2+} oxidation in a stretched c-DN hydrogel based on the Fenton reaction. **a.** Fenton color reaction induced by mechanoradicals. **b.** Optical images of the Fenton color reaction in a c-DN hydrogel induced by mechanoradicals, an aqueous solution of 100 µM $(NH_4)_2Fe^{II}(SO_4)_2$, 250 µM XO and 20 mM H_2SO_4 was used to emphasize the color contrast. **c.** The UV-visible spectra of the stretched gels fed with ferrous ions and XO. The chart underneath reveals the calculation results.
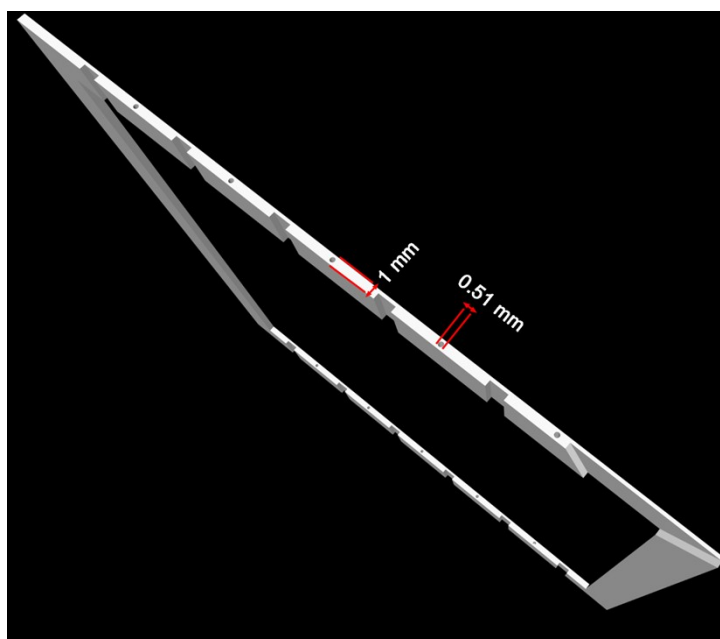
Fabrication of c-DN hydrogels

Figure S2. The square shaped mold: 8 cm×8 cm (wide×length) for fixing capillaries during the curing process of the PNaAMPS hydrogel (first network).
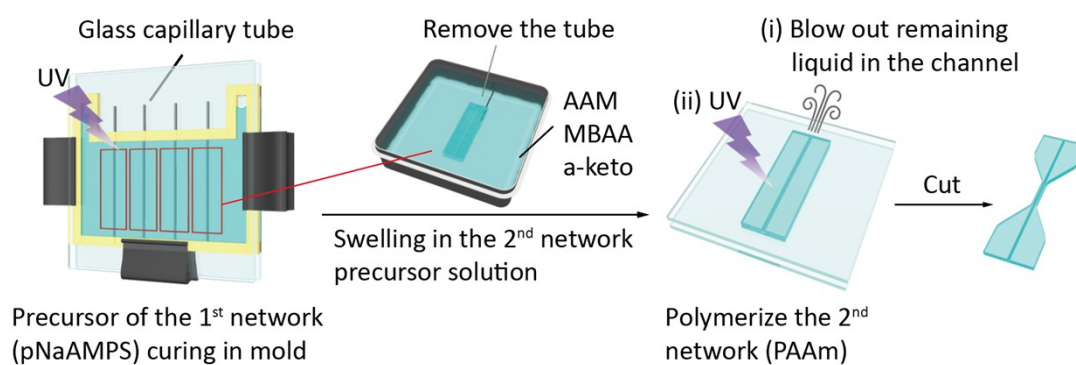

Figure S3. The procedure of using a capillary as the sacrificial mold to construct a channel inside DN hydrogel.
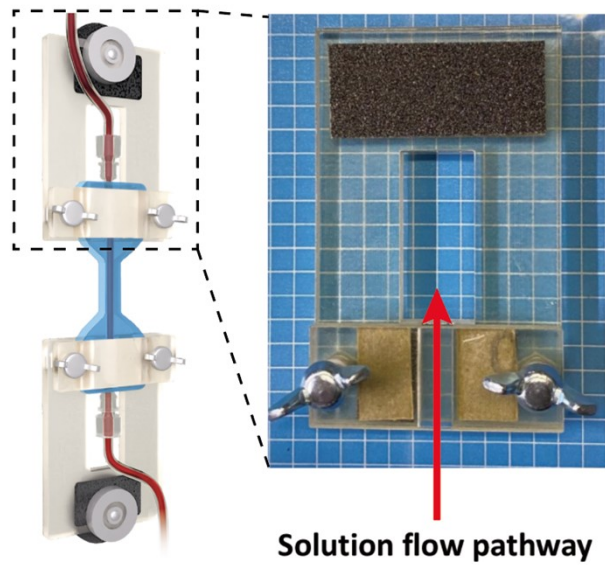
Figure S4. Specially designed jig enabling liquid flow through the channel during stretching.
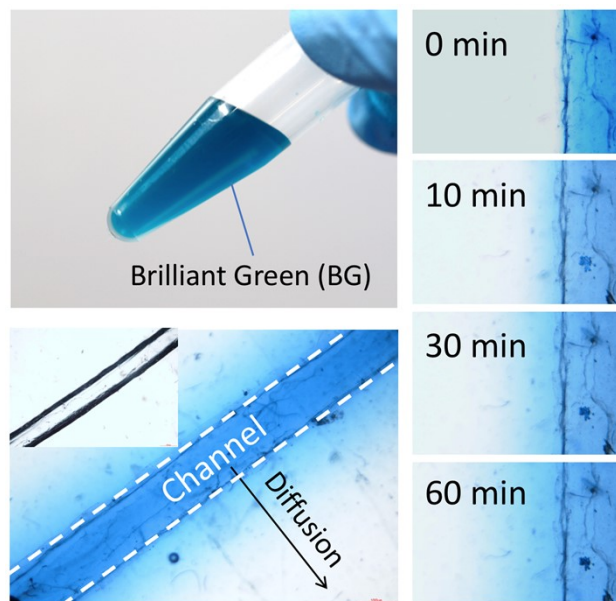

Figure S5. Microscopic optical images to show diffusion of brilliant green molecules from the channel to c-DN hydrogel matrix after various flow times.

ATR FT-IR settings for diffusion measurement.

The absorbance signal of monomers diffusing from the channel to the surface of c-DN gels was detected by an ATR FT-IR spectrometer (FT-IR 6600, Jasco corporation). For measuring the calibration, DN gel slices with the same constitution to the c-DN hydrogel sample were soaked in standard monomer solutions for 2 days. The calibration results of NIPAAm (Fig. S7a) and NaAMPS (Fig. S8a) were used to calculate the monomer concentration change during the circulatory flow. To detect the diffusion kinetics of monomer solution, 0.1 M NaAMPS and 1.0 M NIPAAm solutions were used to perfuse the c-DN hydrogel through the internal channel. The gauge part of the c-DN hydrogel was fixed on the measurement substrate with a close contact to the ATR-IR crystal.
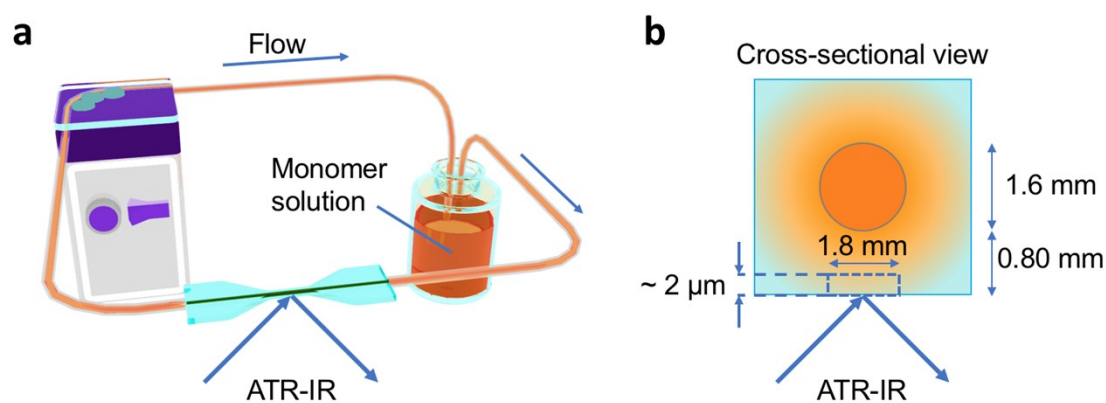

Figure S6. The experimental setup to characterize the diffusion of monomers. **a.** An illustration of the monomer aqueous solution circulation system constructed by c-DN hydrogel, the chemical signals are collected from the gauge part. **b.** Cross-sectional view of the gauge part. The chemical signals were collected from the c-DN hydrogel surface by the ATR-FTIR spectroscopy.
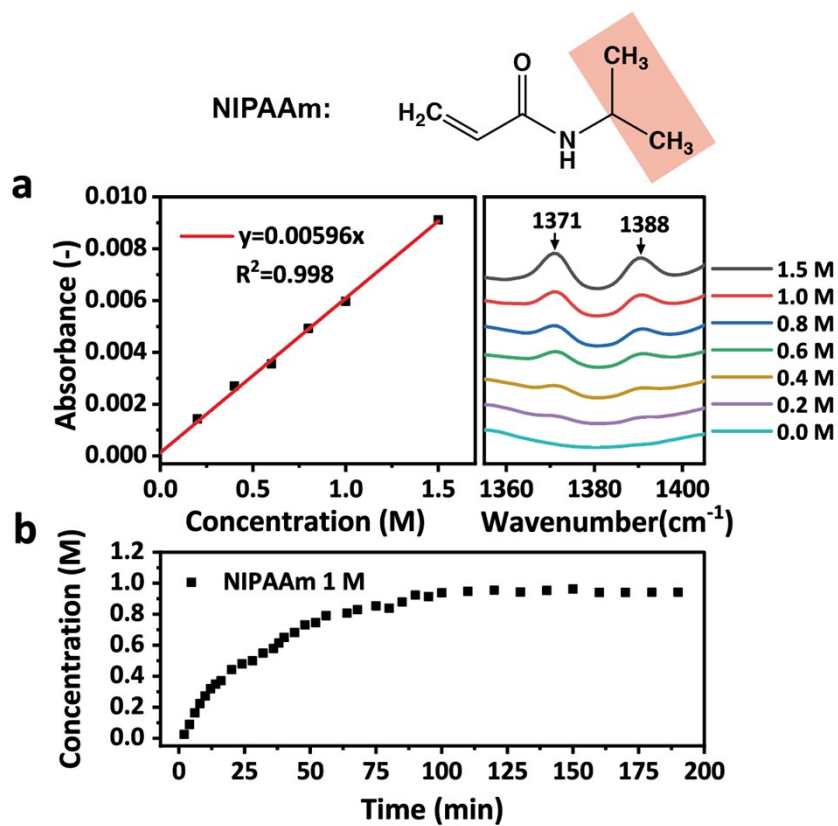
Figure S7. ATR-FTIR results of NIPAAm. **a.** Absorbance collected from peak of 1371 cm^{-1}, spectra were taken from DN hydrogels after soaked in 1.5, 1.0, 0.8, 0.6, 0.4, 0.2, and 0 M standard NIPAAm solutions. **b.** Time profile of concentration of NIPAAm on the surface of c-DN gel (0.8 mm from the circular channel surface) during circulation of 1.0 M NIPAAm aqueous solution.
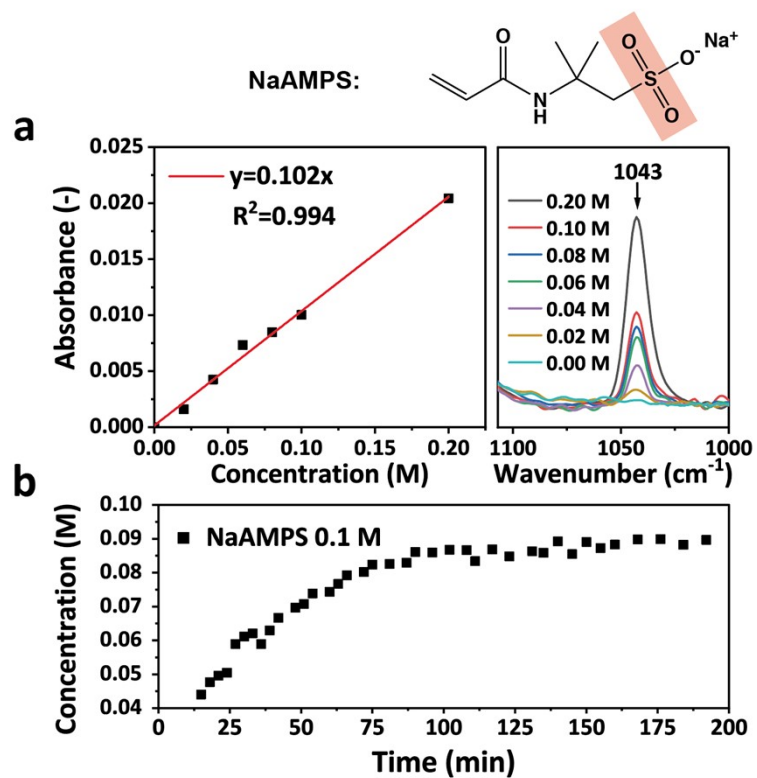
Figure S8. ATR-FTIR spectra results of NaAMPS. **a.** Absorbance collected from peak of 1043 cm^{-1}, spectra were taken from DN hydrogels after soaked in 0.20, 0.10, 0.08, 0.06, 0.04, 0.02, and 0.00 M standard NaAMPS solutions. **b.** Time profile of concentration of NaAMPS on the surface of c-DN gel (0.8 mm from the circular channel surface) during circulation of the 0.1 M NaAMPS aqueous solution.
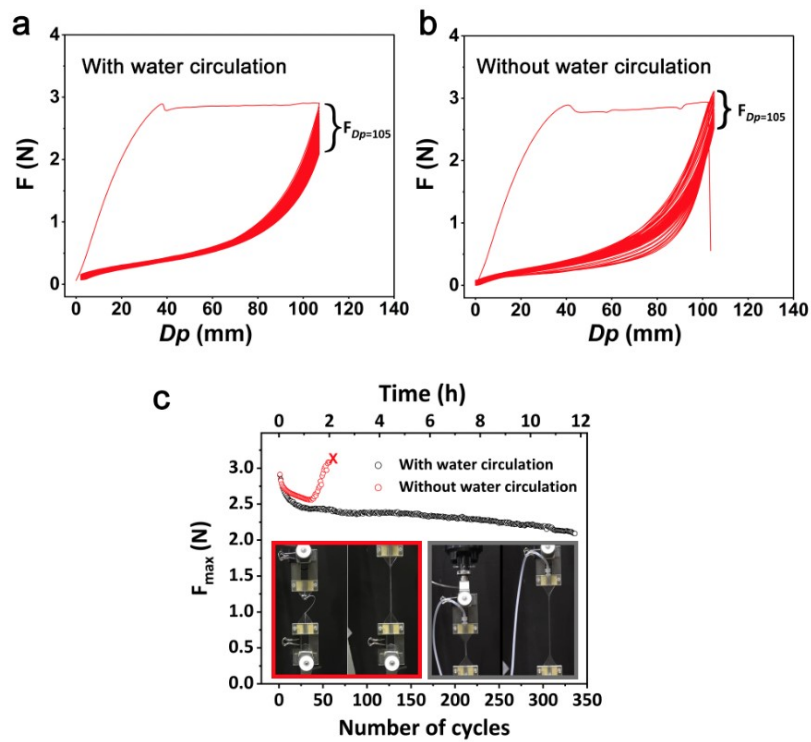
Figure S9. Stability of c-DN hydrogel in open air illustrated by cyclic tensile tests. **a.** With, and **b.** Without continuous water circulation. **c.** Tensile force at a displacement (*Dp*) of 105 mm for the upper jig as a function of cyclic number and time. The inserted images depict the final sample appearances without water circulation (red frame, dry and brittle after 2 h) and with continuous water circulation (black frame, moist and soft after 12 h).
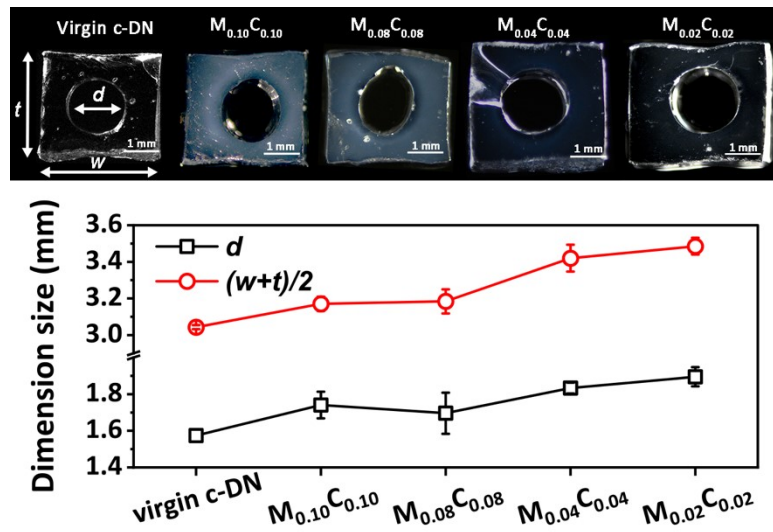
Figure S10. Photographs of the c-DN gel slices supplied with various monomer and crosslinker concentrations and their corresponding cross-sectional size after one tensile cycle, the $M_{0.10}C_{0.10}$ and $M_{0.08}C_{0.08}$ exhibit little swelling owing to the densely cross-linked network.
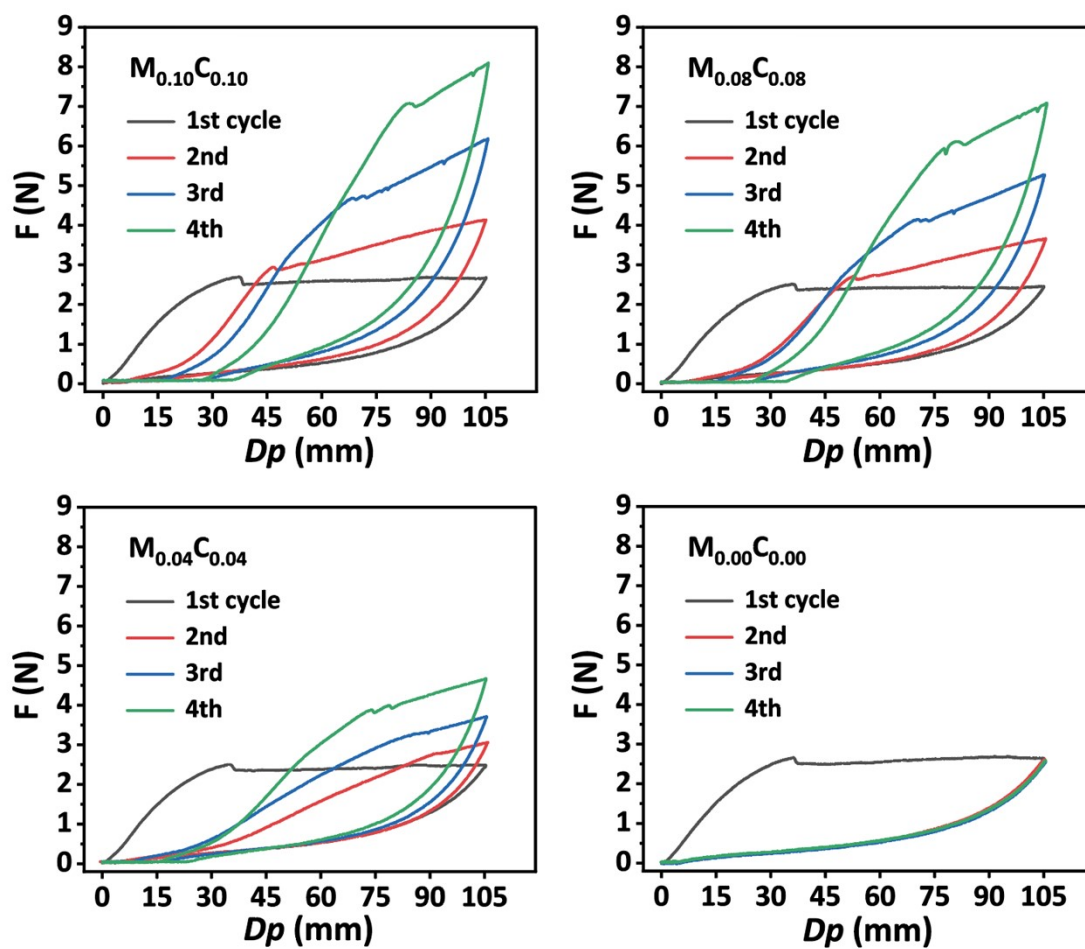
Figure S11. Force–displacement curves of the four times of cyclic loading–unloading under supply of monomers and cross-likers of various concentrations. The results are replotted to the force–time curves in Figure 7a (upper panel).
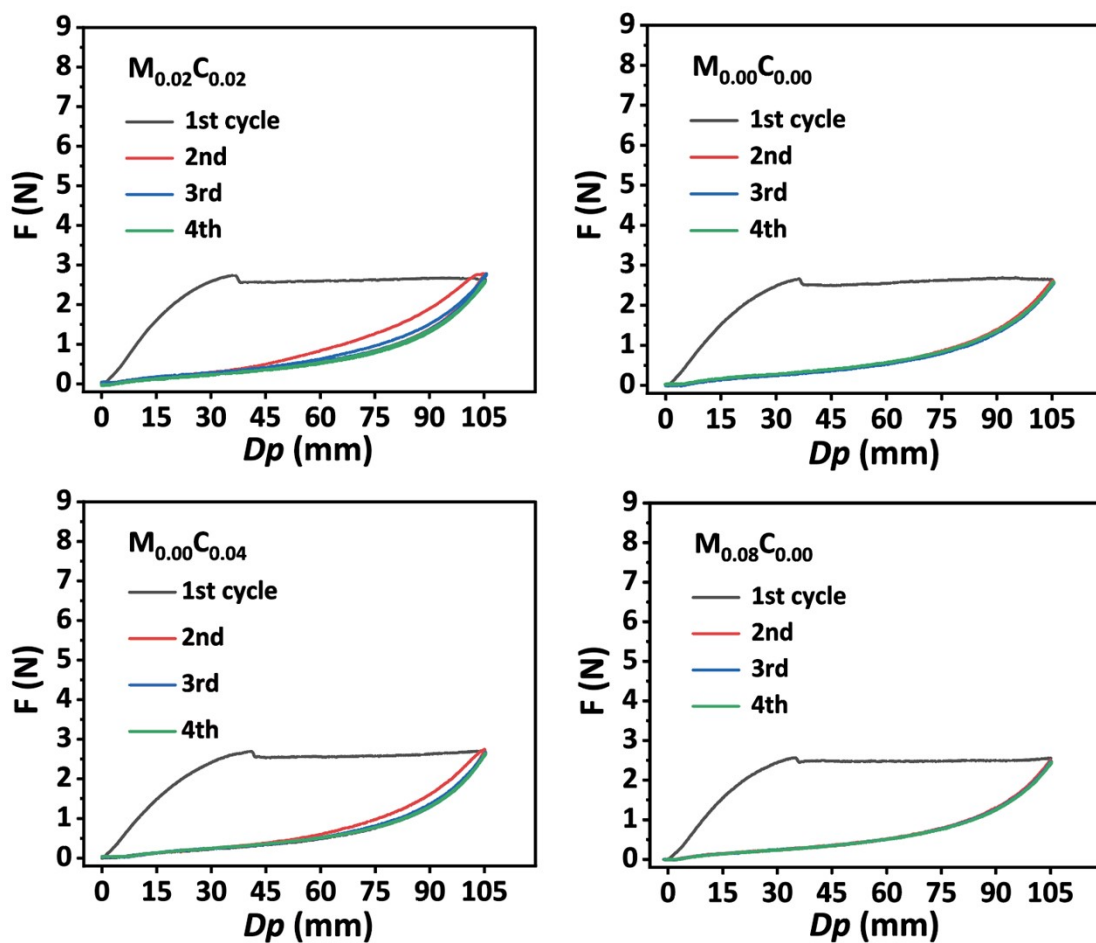
Figure S12. Force–displacement curves of the four times of cyclic loading–unloading under supply of monomers and cross-likers of various concentrations. The results are replotted to the force–time curves in Figure 7a (middle panel).
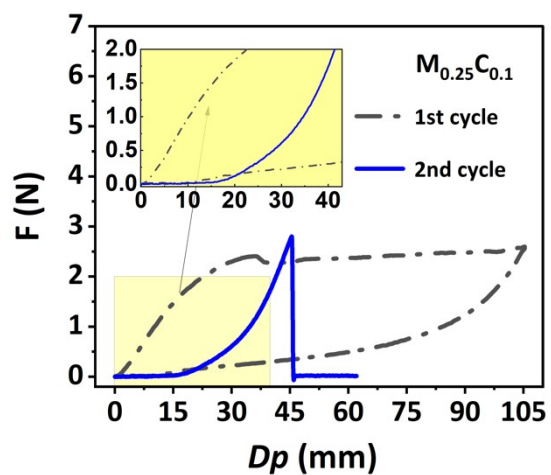
Figure S13. Force–displacement curves of the cyclic loading–unloading in the 1st and 2nd tensile cycle, the c-DN sample was fed with 0.25 mol/L monomer (NaAMPS) and 0.10 mol/L cross-liker (MBAA).
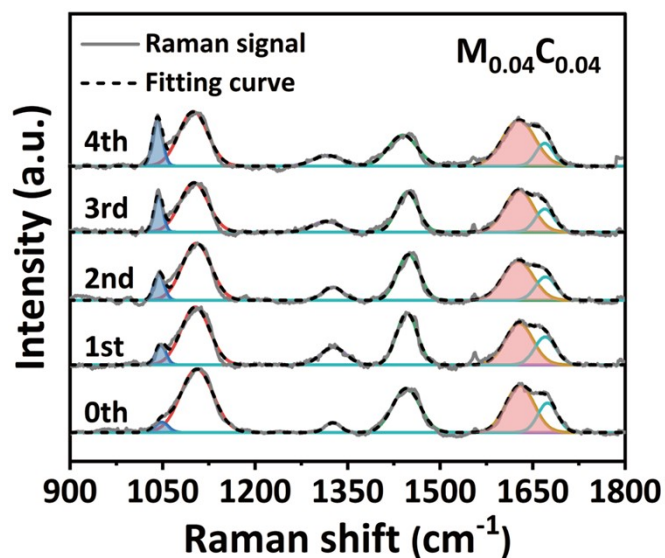
Figure S14. Raman spectroscopy of c-DN samples during four times stretching with simultaneous supply of the solution containing 0.04 M NaAMPS monomer and 0.04 M MBAA cross-linker. The peak at 1045 cm^{-1} corresponds to the S=O stretching in PNaAMPS (marked as blue), and the peak at 1630 cm^{-1} corresponds to the NH$_2$ scissoring in PAAm (marked as red).
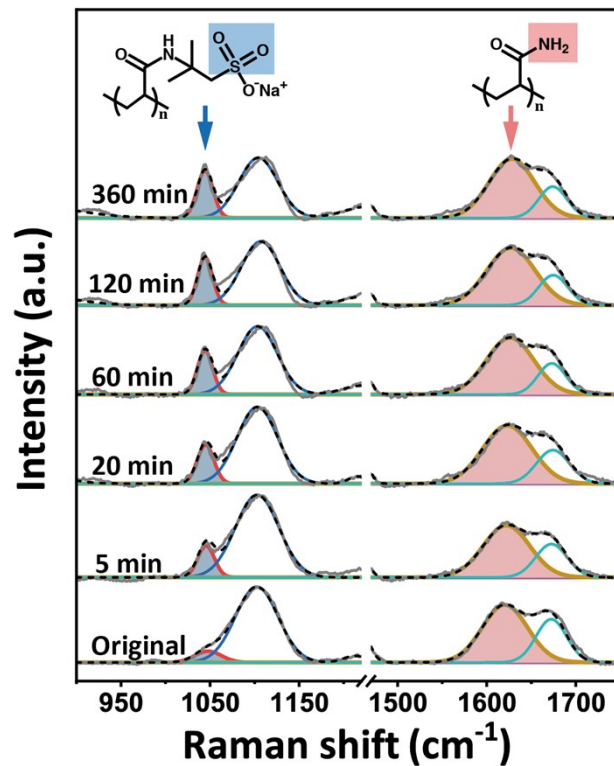
Figure S15. Raman spectroscopy and the fitting curves of the $M_{0.10}C_{0.10}$ samples after the second stretch, the Raman signals of the original gel as a reference, the peaks correspond to PNaAMPS and PAAm is marked as blue and red, respectively.

Table S1 Raman band positions and assignments.

Wavenumber (cm^{-1})	Assignments
1045	S=O stretching[3]
1112	C-C skeletal stretching[4]
1327	CH, NH bending[5, 6]
1457	CH_2 bending[5, 7], CH_3 scissoring[6]
1630	NH_2 scissoring[8-11]
1657	C=O stretching[10, 11]

Movie:

Movie S1: c-DN hydrogel with fluid (dyed in red) flowing through the channel during cyclic tensile stretch.

Movie S2: Muscle-like behaviours of a c-DN hydrogel supplied by 0.10 M NaAMPS monomer and 0.10 M MBAA cross-linker showing repetitive stretch-triggered mechanical growth.

References

1   T. Matsuda, R. Kawakami, R. Namba, T. Nakajima and J. P. Gong, Science, 2019, **363**, 504-508.

2   Z. J. Wang, J. L. Jiang, Q. F. Mu, S. Maeda, T. Nakajima and J. P. Gong, J Am Chem Soc, 2022, **144**, 3154-3161.

3   A. Selvarajan, Proceedings of the Indian Academy of Sciences - Section A, 1966, **64**, 44–50.

4   M. K. Gupta and R. Bansil, J Polym Sci Pol Phys, 1981, **19**, 353-360.

5   J. S. Suh and K. H. Michaelian, J Raman Spectrosc, 1987, **18**, 409-414.

6   P. Bour, J. Kapitan and V. Baumruk, J Phys Chem A, 2001, **105**, 6362-6368.

7   A. I. Jirasek, C. Duzenli, C. Audet and J. Eldridge, Phys Med Biol, 2001, **46**, 151-165.

8   P. L. Anto, R. J. Anto, H. T. Varghese, C. Y. Panicker, D. Philip and A. G. Brolo, J Raman Spectrosc, 2009, **40**, 1810-1815.

9   M. Reichenbächer and J. r. Popp, Challenges in molecular structure determination, Springer, Heidelberg ; New York, 2012.

10 P. G. Puranik and K. V. Ramiah, P Indian Acad Sci A, 1961, A 54, 69-79.

11 F. D'Amico, B. Rossi, G. Camisasca, F. Bencivenga, A. Gessini, E. Principi, R. Cucini and C. Masciovecchio, Phys Chem Chem Phys, 2015, **17**, 10987-10992.